

Proceedings of the XXIII Conference on Applied Crystallography, Krynica Zdrój, Poland, September 20–24, 2015

Structural Characterization of $\text{La}_{1-x}\text{Sr}_x\text{CoO}_3$ Thin Films Deposited by Pulsed Electron Deposition Method

Ł. CIENIEK*, A. KOPIA, A. CYZA, K. KOWALSKI AND J. KUSIŃSKI

AGH University of Science and Technology, Faculty of Metals Engineering and Industrial Computers Science, al. A. Mickiewicza 30, 30-059 Krakow, Poland

The aim of the presented research was to investigate the influence of strontium dopant on the structure and composition of $\text{La}_{1-x}\text{Sr}_x\text{CoO}_3$ ($x = 0, 0.1, 0.2$) perovskite thin films. Pure and Sr doped LaCoO_3 thin films were grown by pulsed electron deposition technique on crystalline epi-polished Si/MgO substrates. Numerous analytical techniques (scanning electron microscopy, atomic force microscopy, X-ray photoelectron spectroscopy, and X-ray diffraction) were applied to characterize their phase/chemical composition, structure and surface morphology. X-ray diffraction analysis showed the presence of pure LaCoO_3 perovskite phase in the undoped thin film. For Sr doped thin films $\text{La}_{0.8}\text{Sr}_{0.2}\text{CoO}_3$ ($x = 0.2$), $\text{La}_{0.9}\text{Sr}_{0.1}\text{CoO}_3$ ($x = 0.1$) small contents of La_2O_3 and LaSrCoO_4 phases were noticed. The crystallite sizes, calculated from the Williamson–Hall plots, were about 18 nm for all analyzed films. According to scanning electron microscopy/atomic force microscopy observations, obtained thin films were free from defects and cracks. Atomic force microscopy (tapping mode) analysis revealed the differences in the shape and quantity of surface crystallites for all thin films as a result of Sr doping and different deposition parameters. Atomic force microscopy technique also allowed measurement of roughness parameters for analyzed samples. X-ray photoelectron spectroscopy analyses of chemical states of elements of thin films showed that their chemical state was stable across the film thickness and even at the interface with the MgO substrate. X-ray photoelectron spectroscopy analysis also allowed to evaluate chemical states and atomic concentration of La, Co, and Sr elements within cross-sections of deposited thin films.

DOI: [10.12693/APhysPolA.130.1121](https://doi.org/10.12693/APhysPolA.130.1121)

PACS/topics: 81.15.-z, 81.10.Bk, 81.07.Bc, 68.55.-a, 68.55.J-, 68.55.Nq, 68.37.-d

1. Experimental procedure

LaCoO_3 based perovskites are known as the functional materials that are widely used especially for electronic and catalytic applications. Unique properties of such materials are often affected by both, the type and the concentration of the dopant (i.e. Fe, Sr, Ca) as well as the parameters of the deposition/manufacturing technique. In this work, the influence of pulsed electron deposition (PED) parameters and Sr dopant concentration on the structure and properties of LaCoO_3 based perovskites thin films is discussed.

$\text{La}_{1-x}\text{Sr}_x\text{CoO}_3$ ($x = 0, 0.1, 0.2$) perovskite thin films were deposited on crystalline epi-polished substrates: (100) oriented Si, and (100) MgO ($10 \times 10 \text{ mm}^2$). The PED system consisting of electron gun PEBS-32 and vacuum chamber Pioneer 180 (manufactured by Neocera) was used for the electron ablation process. The design and operation of PED system was described elsewhere [1]. The experimental setup used in this work for $\text{La}_{1-x}\text{Sr}_x\text{CoO}_3$ ($x = 0, 0.1, 0.2$) thin films production is presented in Table I.

The phases composition of the target and perovskite thin films was examined by means of the X-ray diffraction phase analysis using PANanalytical EMPYREAN DY 1061 with $\text{Cu } K_\alpha$ ($\lambda_{\text{Cu}} = 0.154 \text{ nm}$) radiation in the Bragg–Brentano and grazing geometry. The newest

TABLE I

Parameters of LaCoO_3 and LaSrCoO_3 thin films PED process.

Sample	LaCoO_3	$\text{La}_{0.8}\text{Sr}_{0.2}\text{CoO}_3$	$\text{La}_{0.9}\text{Sr}_{0.1}\text{CoO}_3$
electron energy	10 kV	10 kV	10.5 kV
gap		2.5÷3 mm	
target–substrate dist.	80 mm	80 mm	70 mm
repetition rate	4 Hz	4 Hz	10 Hz
number of shots		54 000	
substrate temp.		570 °C	
work. gas press. p_{O_2}		12 mbar	
C monitor	144.1	142.3	141.5

data base PDF-4+ (product of ICDD) was used for phase identification. The calculation of cell parameters was performed using CellRef software. The surface morphology and chemical composition of all samples were observed/examined with the use of scanning electron microscope (SEM, FEI Nova NanoSEM 450 equipped with EDAX Energy Dispersive Spectroscopy Detector and GENESIS software). Thin films surfaces topography and roughness parameters were investigated using scanning probe microscope (atomic force microscope, AFM) Veeco Dimension®Icon™SPM with NanoScope V controller. The verification of the chemical states of individual elements was carried out by an X-ray photoelectron spectroscopy (XPS) method using the PHI VersaProbe II instrument.

*corresponding author; e-mail: lukasz.cieniek@agh.edu.pl

2. SEM/AFM structure observations

On the basis of thorough structural analysis of pure and Sr doped LaCoO_3 thin films (Fig. 1) it can be concluded that obtained perovskite films are generally dense, compact and free from structural defects (there were no pores and fractures observed). The presence of clusters/agglomerates on perovskite surfaces does not significantly influence their properties. Observed structure, however, is quite different, considering the target composition and PED parameters (electron energy, repetition rate and target-substrate distance). For the $\text{La}_{0.9}\text{Sr}_{0.1}\text{CoO}_3$ thin film (10.5 kV, 10 Hz, 70 mm) one can notice a minor amount of very small droplets. Their diameter does not exceed 0.5 μm . The visible layer (outside droplets) seems to be made of very fine irregularities which may indicate that the growing crystallites are nanometric (Fig. 1e). Meanwhile, on the surface of other two perovskite thin films (10 kV, 4 Hz, 80 mm), a large number of regularly distributed “island-like bulges” can be observed (Fig. 1a,c). It seems that the presence of Sr dopant plays an important role in the formation of surface structure of thin films since the number of clusters/agglomerates is visibly increased for $\text{La}_{0.8}\text{Sr}_{0.2}\text{CoO}_3$ as against LaCoO_3 . The topography study of all perovskite thin films (Fig. 1b,d,f) done by AFM (tapping mode in air) is in agreement with the results obtained at larger scale from SEM analysis (Fig. 1a,c,e). As can be seen, the surface of the $\text{La}_{0.9}\text{Sr}_{0.1}\text{CoO}_3$ thin film is built of very fine irregularities (bulges) that constitute the proper thin film. The droplets, also observed by SEM, are indeed small in size, but their number cannot be ignored. Fine irregularities may be treated as the fronts of growing crystals. As mentioned before the structure (topography) of the prepared thin films differs depending on the target composition as well as the deposition conditions and this is evident in measured roughness values given in Fig. 1.

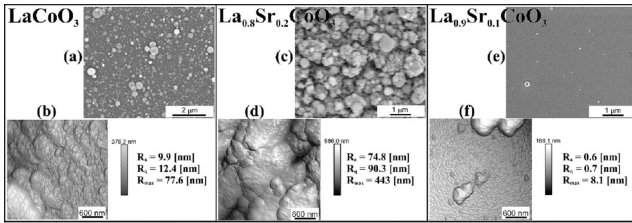


Fig. 1. Images of perovskites thin films surfaces SEM/AFM observations coupled with roughness parameters: (a,b) LaCoO_3 , (c,d) $\text{La}_{0.8}\text{Sr}_{0.2}\text{CoO}_3$, (e,f) $\text{La}_{0.9}\text{Sr}_{0.1}\text{CoO}_3$.

3. X-ray diffraction analysis

Phase composition of the target was studied by X-ray diffraction method in the Bragg-Brentano geometry. In the target we observed only LaCoO_3 , $\text{La}_{0.9}\text{Sr}_{0.1}\text{CoO}_3$, and $\text{La}_{0.7}\text{Sr}_{0.3}\text{CoO}_3$

with a minor amount of LaSrCoO_4 . The analysis of thin films was performed in grazing geometry at the angle $\alpha = 1^\circ$. The results are shown in Fig. 2. The phase identification was based on the JCPDS base cards: (00-025-1060) LaCoO_3 , (01-089-4457) $\text{La}_{0.7}\text{Sr}_{0.3}\text{CoO}_3$, (01-083-1344) La_2O_3 , (01-083-2410) LaSrCoO_4 . The analysis of diffraction patterns obtained for thin films revealed the presence of La_2O_3 and LaSrCoO_4 phases (low content). Based on the X-ray results determined from the Williamson-Hall plot the average crystallite size for each film was calculated. For calculation we used only peaks as follows: (012), (110), (104), (024), (300), (214), (018). The crystalline size were about 18 nm approximately the same for all thin films. We did not observe the decrease of the crystalline size with doping by Sr. Doping of the perovskite by other elements may result in slowing of the crystal growth process [2] or the blockade of crystal growth, causing the grain's fragmentation. Diffraction patterns for doped thin films (Fig. 2b,c) showed small shift of diffraction lines (individual peaks) towards higher values of 2θ . LaCoO_3 perovskite has rhombohedral symmetry (space group $R3c$ (167)) (hexagonal setting) [JCPDS 00-025-1060] (see Table II). $\text{La}_{1-x}\text{Sr}_x\text{CoO}_3$ has the same rhombohedral structure in the range of $x = 0 \div 0.5$ for Sr. For values of $x > 0.5$ the system becomes cubic [3]. In our case, the volume of the cell changed with the increase of the Sr dopant (Table II). Similar effects were observed in the system of LaCoO_3 doped by K [4] or Ba [5]. Observed changes of the cell volume are not the consequence of Sr^{2+} substitution by La^{3+} . Both La^{3+} (1.36 Å) and Sr^{2+} (1.32 Å) ions have approximately the same size. However, in order to preserve the electro-neutrality upon the substitution, an increase of the cobalt oxidation state from Co^{3+} to Co^{4+} must occur and/or oxygen vacancies must be generated. The differences in the ionic radius of cobalt (6-coordinate, octahedral, high spin) in different oxidation states explain the change in the cell volume: Co^{3+} (0.75 Å) and Co^{4+} (0.67 Å). In other words, the change in the cell volume is a direct effect of the existence of some cobalt in oxidation state (IV) and consequently confirms its presence. The evolution of the volume cell was observed by Pecchi [6] in the system of Ca doped LaFeO_3 , where Ca substituted La and Fe was observed in two oxidation states Fe^{3+} and Fe^{4+} .

TABLE II

Structural parameters for Sr^{2+} doped $\text{La}_{1-x}\text{Sr}_x\text{CoO}_3$ ($x = 0 \div 0.2$) perovskites. Crystal system space group is rhombohedral $R3c$ -167; $\alpha, \beta = 90^\circ$, $\gamma = 120^\circ$. For La and Sr $x = y = 0$, $z = 0.25$, for Co $x = y = z = 0$

Sample	Lattice parameters [nm]			O		
	$a = b$	c	vol. [nm^3]	x	y	z
$x = 0$	0.5449	1.310	33.698	0.4537	0	0.25
$x = 0.1$				0	0	0.25
$x = 0.2$	0.5454	1.313	33.85	0.4554	0	0.25

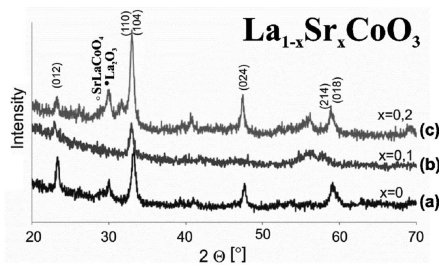


Fig. 2. X-ray patterns in grazing geometry $\alpha = 1^\circ$ of thin films: (a) LaCoO_3 , (b) $\text{La}_{0.9}\text{Sr}_{0.1}\text{O}_3$, (c) $\text{La}_{0.8}\text{Sr}_{0.2}\text{CoO}_3$.

4. XPS experimental

XPS analyses coupled with the Ar^+ ion sputtering were used to investigate the oxidation state of elements on the surface, inside the films at different depth as well as at the film/substrate interfaces in order to find whether the elements from the thin film reacted or did not with the substrate. First XPS analysis of each sample was made on the as received thin film surface. Then the samples were sputtered using the Ar^+ ion beam (ion etching) during the certain time and after the sputtering process they were immediately analyzed using XPS. The process of sputtering and subsequent XPS analysis was repeated for all samples several times until the substrate of the coating was reached. Chemical states of the perovskite thin film and substrate elements were investigated by registering their strongest spectral lines: La $3d$, Co $2p$, Sr $3d$, O $1s$, and Mg $1s$ (Fig. 3). On the surface of both samples (LaCoO_3 , $\text{La}_{0.8}\text{Sr}_{0.2}\text{CoO}_3$) besides the component elements of the films, there was detected the presence of an adventitious carbon (monitored line C $1s$) and the adventitious oxygen. They constitute the surface contamination. For both thin films after the first sputtering process the spectral line of carbon and the spectral line of the adventitious oxygen completely disappeared and were also absent after every further sputtering process.

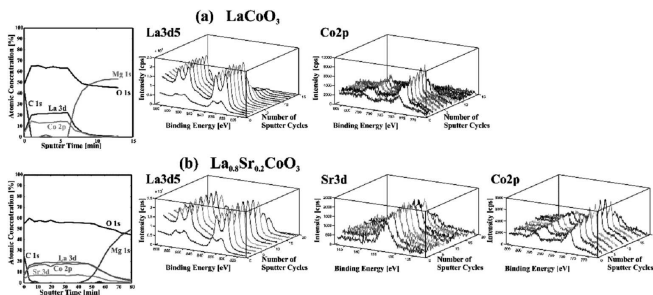


Fig. 3. XPS analysis results for (a) LaCoO_3 and (b) $\text{La}_{0.8}\text{Sr}_{0.2}\text{CoO}_3$ thin films.

5. Concluding remarks

The PED process enables to produce good quality thin films of crystalline LaCoO_3 and LaSrCoO_3 perovskites on $[001]$ Si /MgO substrates that was confirmed by SEM/AFM observations coupled with roughness parameters measurements. Morphology of analyzed films is highly influenced by the PED parameters like electron energy (accelerating voltage), target–substrate distance, and pulse repetition rate. Except the surface (contamination by the adventitious carbon and oxygen), XPS analyses of chemical states of elements of thin films showed that their chemical state was stable across the film and even at the interface with the substrate. For LaSrCoO_3 perovskites unit cell volumes were slightly increased (compared to pure LaCoO_3), that is the consequence of either the cobalt oxidation state changes (Co^{3+} to Co^{4+}) and/or oxygen vacancies appearance. Diffraction patterns for Sr doped LaCoO_3 thin films showed the small shift of diffraction lines (individual peaks) to the right towards higher values of the 2θ . The average crystallite size was calculated ≈ 18 nm for all thin films regardless of the presence of Sr dopant. Analyzed diffraction patterns revealed small content of La_2O_3 and LaSrCoO_4 phases for Sr doped LaCoO_3 films.

Acknowledgments

This work is supported by the National Science Centre (grant no. UMO-2013/09/B/ST8/01681).

References

- [1] M.D. Strikovski, J. Kim, S.H. Kolagani, in: *Springer Handbook of Crystal Growth*, Eds. G. Dhanaraj, K. Byrappa, V. Prasad, M. Dudley, Springer, Berlin 2010, p. 1193.
- [2] S. Phokha, S. Hunpratup, S. Pinitsoontorn, B. Putasaeng, S. Rujirawat, S. Maensiri, *Mater. Res. Bull.* **67**, 118 (2015).
- [3] N. Orlovskaya, K. Kleveland, T. Grande, M.A. Einarsrud, *J. Eur. Ceram. Soc.* **20**, 51 (2000).
- [4] B.M. Bellakki, C. Madhu, T. Greindl, S. Kohli, P. McCurdy, V. Manivannan, *Rare Met.* **29**, 491 (2010).
- [5] R. Kun, S. Populoh, L. Karvonen, J. Gumbert, A. Weidenkaff, M. Busse, *J. Alloys Comp.* **579**, 147 (2013).
- [6] G. Pecchi, M.G. Jiliberto, A. Buljan, E.J. Delgado, *Solid State Ion.* **187**, 27 (2011).